

Photo-induced formation and self-assembling of gold nanoparticles in aqueous solution of amphiphilic dendrimers with oligo(*p*-phenylene vinylene) core branches and oligo(ethylene oxide) terminal chains

This article has been downloaded from IOPscience. Please scroll down to see the full text article.

2007 Nanotechnology 18 365605

(<http://iopscience.iop.org/0957-4484/18/36/365605>)

View [the table of contents for this issue](#), or go to the [journal homepage](#) for more

Download details:

IP Address: 129.22.126.46

The article was downloaded on 03/01/2012 at 18:14

Please note that [terms and conditions apply](#).

Photo-induced formation and self-assembling of gold nanoparticles in aqueous solution of amphiphilic dendrimers with oligo(*p*-phenylene vinylene) core branches and oligo(ethylene oxide) terminal chains

Dong Wook Chang and Liming Dai¹

Department of Chemical and Materials Engineering and Chemistry, School of Engineering and UDRI, University of Dayton, 300 College Park, Dayton, OH 45469, USA

E-mail: ldai@udayton.edu

Received 23 April 2007, in final form 29 June 2007

Published 14 August 2007

Online at stacks.iop.org/Nano/18/365605

Abstract

Dendritic molecules with oligo(*p*-phenylenevinylene) core branches and oligo(ethylene oxide) terminal chains were found to be highly susceptible to the singlet oxygen mediated photooxidation process. These photosensitive amphiphilic dendrimers were used as both the photo-reducing agent and particle stabilizer for the formation of gold nanoparticles in an aqueous solution of hydrogen tetrachloroaurate (III) hydrate ($\text{HAuCl}_4 \cdot 3\text{H}_2\text{O}$) at ambient atmosphere. Gold nanoparticles produced at high molar ratios of the amphiphilic dendrimer to HAuCl_4 (>0.5) were demonstrated to be stable for several months, whereas relatively large hexagonal/triangular gold single-crystal films and self-assembled hollow fiber clusters were observed at lower molar ratios of the amphiphilic dendrimer to HAuCl_4 .

(Some figures in this article are in colour only in the electronic version)

1. Introduction

Metal particles are known to be useful for a wide range of applications. For instance, the use of silver particles in photography has been studied for generations [1]. The recent discovery of the size-/shape-dependent properties associated with nanoparticles generated considerable renewed interest in various metal nanoparticles [2]. One of the major techniques used for producing metal nanoparticles is the chemical reduction of metal salts in solution [3]. The solution reduction method has long been used to produce various shape-controlled metal nanoparticles, including Ag [4], Fe [5], Ge [6], Cr [7], Cu [8], Pt [9], and Au [10]. Among them, Au nanoparticles have been most widely investigated due to their unique optical,

electrical and other properties [11]. Several synthetic routes have been devised to control the size and shape of gold nanoparticles [10–12]. Owing to its simplicity and versatility, the chemical reduction of gold (III) salts in a liquid phase using reducing agents, such as sodium borohydride, sodium citrate, hydrogen and alcohol derivatives, has been most widely studied [12, 13].

Like most other colloidal particles [14], the unprotected Au nanoparticles produced from the chemical reduction are normally unstable and show a strong tendency for aggregation. Therefore, some particle stabilizer(s) need to be added into the reduction medium to avoid undesirable aggregation. Particle stabilizers, typically having a portion of their molecular structure anchored (either chemically or physically) on the nanoparticle surface with the remaining part dan-

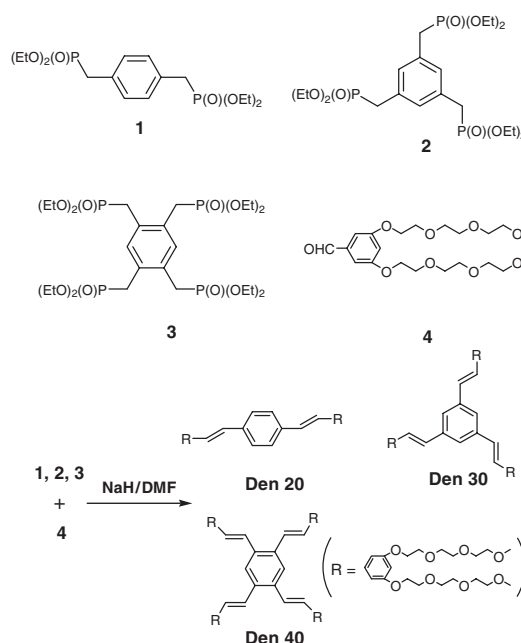
¹ Author to whom any correspondence should be addressed.

gling into the solvent, include thiols [15], surfactants [16], polymers [17, 20–22], and dendrimers [18]. Certain macromolecules, such as amine-terminated poly(propyleneimine) dendrimers [19], π -conjugated polymer [20], poly(ethylene glycol) (PEO) [21], and poly(ethylene oxide)–poly(propylene oxide)–poly(ethylene oxide) block copolymer [22], have been shown to act as not only the particle stabilizer for preventing nanoparticles from aggregation but also the reducing agent for the nanoparticle formation. The use of such dual-function materials can effectively eliminate by-product generation from the reducing agent in the multi-step nanoparticle preparation associated with the more conventional reduction process. In addition to the chemical reduction of metal salts with reducing agents, various synthetic strategies like thermal [23], photochemical [24], sonochemical [25], and electrochemical [26] approaches have also been developed for the preparation of nanoparticles. Among them, the photochemical approach is of particular interest as it is very convenient, energy saving and environmentally friendly.

On the other hand, conjugated poly(*p*-phenylene vinylene) (PPV), oligo(*p*-phenylene vinylene) (OPV), and their derivatives have attracted a great deal of interest as a class of the most promising optoelectronic materials since the first report of electroluminescence from PPV in 1990 [27, 28]. In this context, we have previously reported the preparation and aggregation of amphiphilic light-emitting dendrons consisting of hydrophobic oligo(*p*-phenylene vinylene) core branches and hydrophilic oligo(ethylene oxide) terminal chains [29]. Like most other conjugated structures, PPV moieties are susceptible to photooxidation [30]. As a consequence, singlet oxygen species were generated through a non-radiative decay process by energy transfer from the photo-induced triplet excitons to surrounding oxygen molecules [31]. The singlet oxygen electrophile thus produced can then cause chain scission of the electron-rich conjugated segments to produce α -hydroxy methyl radicals [32], which can act as a reducing agent (*vide infra*). In this paper, we report the dual function of a class of recently synthesized dendritic molecules with hydrophobic oligo(*p*-phenylene vinylene) core branches and hydrophilic oligo(ethylene oxide) terminal chains as both the photo-reducing agent for gold nanoparticle formation and the protecting agent for stabilizing/controlled self-assembling of the resultant gold nanoparticles.

2. Experimental details

Scheme 1 shows the synthetic procedures for preparing the dendritic molecules of oligo(*p*-phenylene vinylene) core branches and oligo(ethylene oxide) terminal chains (designated as **Den 20**, **Den 30**, and **Den 40**) used in the present study. The detailed synthesis and characterization has been reported elsewhere [33]. Briefly, we synthesized the core structures (**1**, **2**, **3**, scheme 1) by Wohl–Ziegler bromination of hydrocarbon moieties with *N*-bromosuccinimide, followed by reaction with triethyl phosphite according to the reported procedure [34, 35]. The aldehyde-functionalized periphery **4** (scheme 1) was synthesized via the Mitsunobu reaction between 3,5-dibromobenzaldehyde and tri(ethylene glycol) monomethyl ether, as we reported earlier [29]. Finally, the Horner–Wadsworth–Emmons coupling reaction was used to



Scheme 1. Procedures for the synthesis of the amphiphilic dendrimers with oligo(*p*-phenylene vinylene) core units and oligo(ethylene oxide) terminal chains.

attach the aldehyde-functionalized periphery **4** onto the respect core structures (**1**, **2**, and **3**), resulting in the formation of **Den 20**, **Den 30** and **Den 40** (scheme 1). The dendritic molecules thus prepared show strong fluorescent emission originating from the OPV core branches whilst their oligo(ethylene oxide) terminal chains impart a good solubility for the whole dendritic molecule in water and common organic solvents (e.g. ethanol, chloroform, Tetrahydrofuran (THF)).

HAuCl₄·3H₂O was purchased from Alfa Aesar. Deionized ultra-filtered water from Fischer Scientific Co. was used for all preparations, and all glassware was cleaned with aqua regia prior to use. In a typical experiment, gold nanoparticles were synthesized by adding 0.2 ml of 8.13 × 10⁻⁴ mol l⁻¹ HAuCl₄·3H₂O solution to approximately 1.8 ml of an aqueous solution of each of the dendrimers at a predetermined concentration in a quartz cuvette at room temperature under the ambient laboratory white light or dark.

Ultraviolet–visible (UV–vis) spectra were measured using a Perkin-Elmer Lambda 900 UV/VIS/NIR spectrometer while photoluminescence spectra were recorded on a Perkin-Elmer LS 55 spectrometer. Transmission electron microscopy (TEM) and electron diffraction (ED) were performed on a Hitachi H-7600 transmission electron microscope at an accelerating voltage of 100 kV. TEM samples were prepared by dropping a droplet of the *as-synthesized* gold nanoparticle solution onto a carbon-coated copper grid (200–300 mesh, Ted Pella) and dried at ambient atmosphere. Scanning electron microscopy (SEM) images were taken on a Hitachi S-4800 high resolution scanning electron microscope. Energy-dispersive x-ray analysis (EDX) for drop-cast gold nanoparticles on a Si wafer was performed on a Zeiss EVO-50XVP environmental SEM instrument equipped with an EDAX detector and Genesis 2000 software.

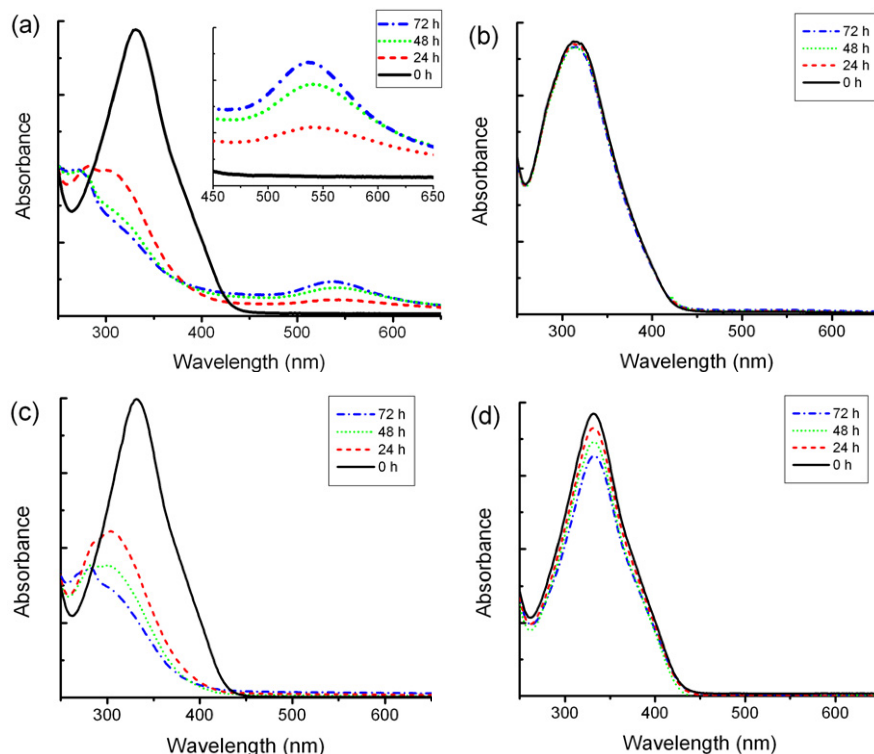
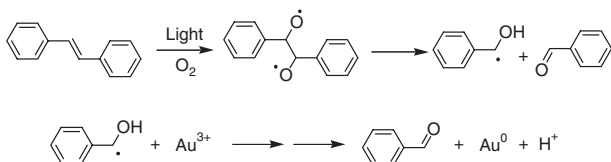


Figure 1. Time dependence of the UV-vis absorption spectra for the mixture of $\text{HAuCl}_4 \cdot 3\text{H}_2\text{O}$ with **Den 40** (a) under light and (b) in the dark; and a pure **Den 40** solution (c) under light and (d) in the dark. The concentrations of $\text{HAuCl}_4 \cdot 3\text{H}_2\text{O}$ and **Den 40** are 8.13×10^{-5} and $4.20 \times 10^{-5} \text{ mol l}^{-1}$, respectively. The inset of (a) shows an enlarged view of the absorption band over 535 nm. Note that the normal laboratory white light was used and all experiments were carried out at room temperature.

3. Results and discussion

Figures 1(a) and (b) show the time evolution of UV-vis absorption spectra for a mixture solution of $\text{HAuCl}_4 \cdot 3\text{H}_2\text{O}$ and **Den 40** in water under light and in the dark, respectively. As can be seen in figures 1(a), a strong absorption peak at $\sim 320 \text{ nm}$ attributable to **Den 40** was observed before exposure to light. Photo-irradiation caused a continuous decrease in the absorption intensity corresponding to the **Den 40** absorption peak, which was accompanied by the appearance of a new absorption band centered at 535 nm with a steady increase in its peak intensity. The newly observed absorption band arises from the characteristic surface plasmon band of gold nanoparticles due to the collective oscillation of electron gas at the nanoparticle surface [36]. Therefore, the appearance of the surface plasmon band reveals the generation of gold nanoparticles in the $\text{HAuCl}_4 \cdot 3\text{H}_2\text{O}$ and **Den 40** mixture system under light.

In view of the oxygen biradical and α -hydroxy methyl radical produced by the above photo-degradation reactions [32], we envisioned that the formation of Au nanoparticles in the present study resulted from the reduction of Au^{3+} ions by the photo-generated reducing agent of α -hydroxy methyl radicals.



The above scenario was supported by a control experiment with the same aqueous solution of $\text{HAuCl}_4 \cdot 3\text{H}_2\text{O}$ and **Den 40** having been kept in the dark, which showed no obvious change in UV-vis absorption (figure 1(b)). Additional control experiments were performed, where the pure **Den 40** solution was kept under light (figure 1(c)) and in the dark (figure 1(d)), respectively. While figure 1(c) shows similar changes as figure 1(a), but without the appearance of the characteristic surface plasmon band for gold nanoparticles, figure 1(d) reveals no obvious change in UV-vis absorption. The difference seen in figures 1(c) and (d) clearly indicates, once again, the photo-degradation of **Den 40**.

Further evidence for the photo-induced formation of gold nanoparticles in the presence of **Den 40** comes from UV-vis absorbance measurements on aqueous solutions of $\text{HAuCl}_4 \cdot 3\text{H}_2\text{O}$ and **Den 40** with different ratios of HAuCl_4 to **Den 40** at a constant **Den 40** concentration under light. Figure 2(a) clearly shows a red-shift and broadening effect for the surface plasmon resonance band with increasing $\text{HAuCl}_4 \cdot 3\text{H}_2\text{O}$ concentration. As the nanoparticle plasmon resonance absorption depends strongly on the particle size [36–38], the directly proportional relationship between the surface plasmon resonance wavelength and the $\text{HAuCl}_4 \cdot 3\text{H}_2\text{O}$ concentration shown in figure 2(b) indicates a gradual size increase for the resultant gold nanoparticles with increasing $\text{HAuCl}_4 \cdot 3\text{H}_2\text{O}$ concentration. A concomitant increase in the population of nanoparticles with different sizes broadened the particle size distribution, leading to relatively broad UV-vis spectra for solutions of higher $\text{HAuCl}_4 \cdot 3\text{H}_2\text{O}$ concentrations (figure 2(a)).

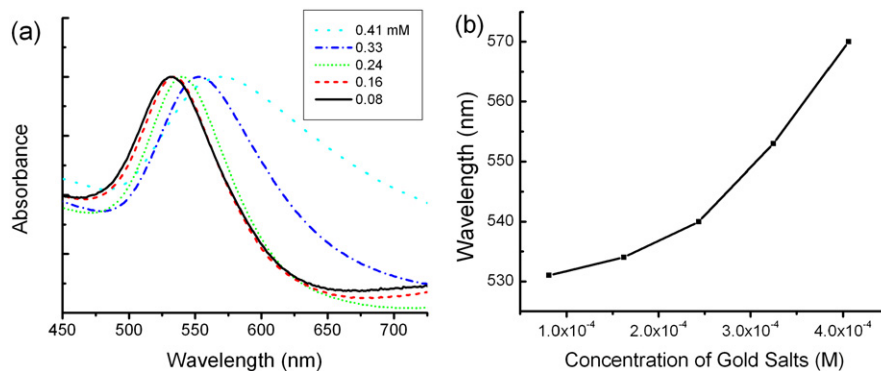


Figure 2. (a) UV-vis spectra of gold nanoparticles at different concentration of the gold salt and (b) the concentration dependence of the wavelength for the maximum surface plasmon band. $[\text{HAuCl}_4 \cdot 3\text{H}_2\text{O}] = 8.13\text{--}40.60 \times 10^{-5} \text{ mol l}^{-1}$, and $[\text{Den 40}] = 4.20 \times 10^{-5} \text{ mol l}^{-1}$.

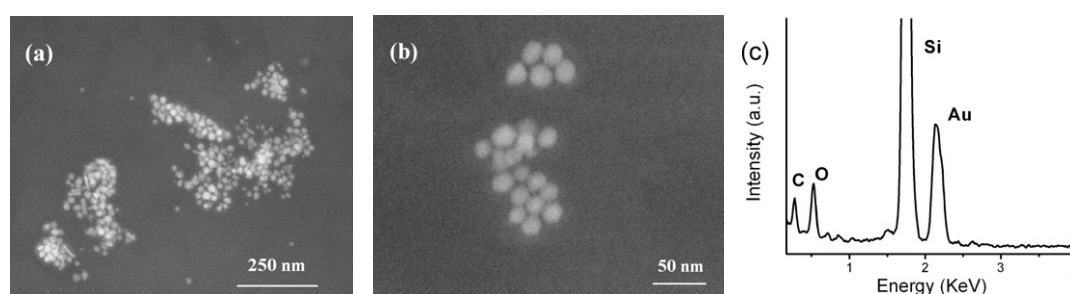


Figure 3. ((a), (b)) SEM images under different magnifications, and (c) EDX data for gold nanoparticles prepared from an aqueous solution of $\text{HAuCl}_4 \cdot 3\text{H}_2\text{O}$ and **Den 40** with concentration of 8.13×10^{-5} and $4.20 \times 10^{-5} \text{ mol l}^{-1}$, respectively.

Figure 3(a) shows a typical SEM image for the resultant gold nanoparticles formed in an aqueous solution of $\text{HAuCl}_4 \cdot 3\text{H}_2\text{O}$ ($8.13 \times 10^{-5} \text{ mol l}^{-1}$) and **Den 40** ($4.20 \times 10^{-5} \text{ mol l}^{-1}$). The corresponding SEM image under a higher magnification given in figure 3(b) reveals a polyhedral geometry, with an average size of about 20 nm for the gold nanoparticles. These gold nanoparticles were found to be stable in the aqueous phase even for several months without precipitation, due, most probably, to adsorption of the residual dendrimers and/or photodegraded dendritic fragments on some of the facets of the polyhedral gold nanoparticles. The energy dispersive x-ray analysis (EDX) of gold nanoparticles on a silicone substrate (figure 3(c)) showed a strong Au signal, along with weak carbon and oxygen peaks originating from the amphiphilic dendritic moieties that bound to the surface of the gold nanoparticles. The adsorbed peripheral OPVs (oligo(*p*-phenylenevinylenes) should play a role in assembling of the resultant gold nanoparticles (*vide infra*), apart from stabilizing of the nanoparticles [39, 40].

The possibility for the peripheral OPV-regulated self-assembling of the gold nanoparticles was checked by photoluminescence (PL) measurements. Figure 4 shows the time dependence of PL spectra for an aqueous mixture solution of $\text{HAuCl}_4 \cdot 3\text{H}_2\text{O}$ and **Den 40** under light (figure 4(a)) and in the dark (figure 4(b)). Similar changes as in the UV-vis spectra (cf figures 1(a) and (b)) were observed for the PL spectra. The observed continuous decrease in the PL emission intensity with time for the aqueous mixture solution of $\text{HAuCl}_4 \cdot 3\text{H}_2\text{O}$ and **Den 40** under light (figure 4(a)) indicates, most probably, the formation/aggregation of Au nanoparticles,

leading to intermolecular photoluminescent quenching for the surface-bonded amphiphilic dendritic moieties. The nanoparticle aggregation could also force the surface-bonded amphiphilic dendritic moieties to adopt a more compact molecular conformation. This, together with the photo-induced chain scission, is responsible for the blue-shift in the PL spectra seen in figure 4(a).

In contrast, figure 4(c) shows an initial increase in PL emission intensity for an aqueous solution of pure **Den 40** under light, which, once again, suggests photo-induced chain scissions to produce more chromophore centers. Further exposure to the ambient light caused a subsequent decrease in PL emission intensities (figure 4(c)) due to the substantial degradation at the late stages. As expected, the massive scission of conjugated segments is accompanied by a blue-shift in the PL peak. No obvious change in PL spectra was observed for the same aqueous solution of pure **Den 40** in the dark (figure 4(d)), in consistency with the UV-vis measurement (figure 1(d)). Similar changes in UV-vis and PL spectra were observed for **Den 20** and **Den 30**, with and without the presence of HAuCl_4 .

To further study the peripheral OPV-induced stabilizing/self-assembling of the gold nanoparticles, we proceeded to examine the stability of gold nanoparticles formed in aqueous solutions with different ratios of **Den 40** to HAuCl_4 at different component concentrations under light. We found that the gold nanoparticles prepared at a relatively high ratio of **Den 40** to HAuCl_4 (>0.5 , figure 3) are very stable in the preparation solution without any precipitation for several months. However, a large amount of dispersed polyhedral

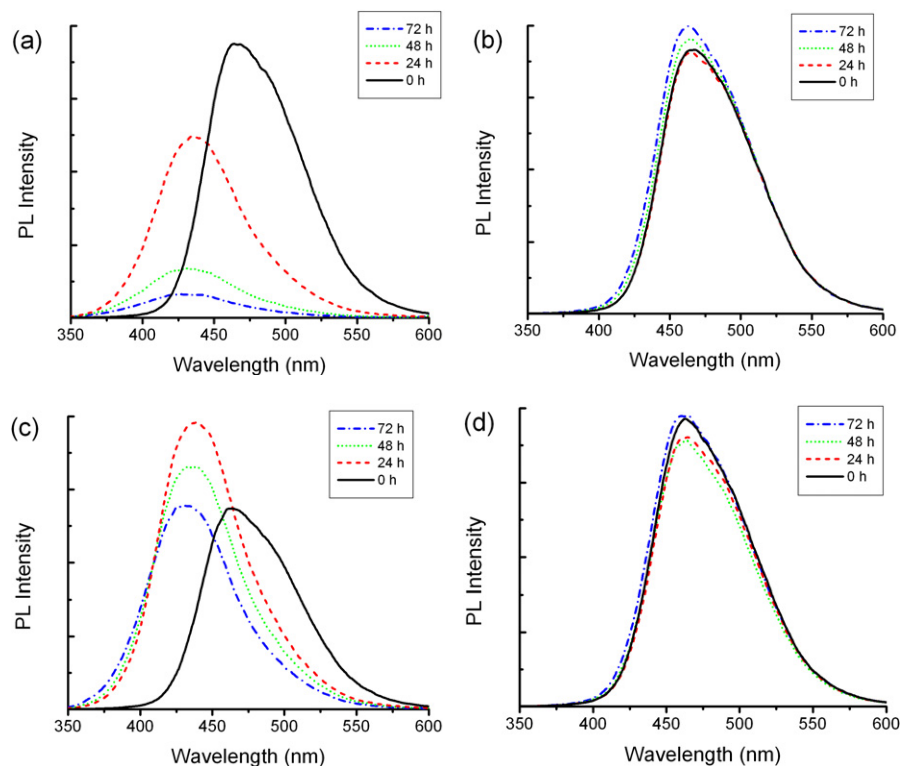


Figure 4. Time-dependent photoluminescent spectra of the mixture of $\text{HAuCl}_4 \cdot 3\text{H}_2\text{O}$ and **Den 40**: (a) under light and (b) in the dark; and a pure **Den 40** solution: (c) under light and (d) in the dark. The concentrations of $\text{HAuCl}_4 \cdot 3\text{H}_2\text{O}$ and **Den 40** are 8.13×10^{-5} and $4.20 \times 10^{-5} \text{ mol l}^{-1}$, respectively. The excitation wavelength is 310 nm.

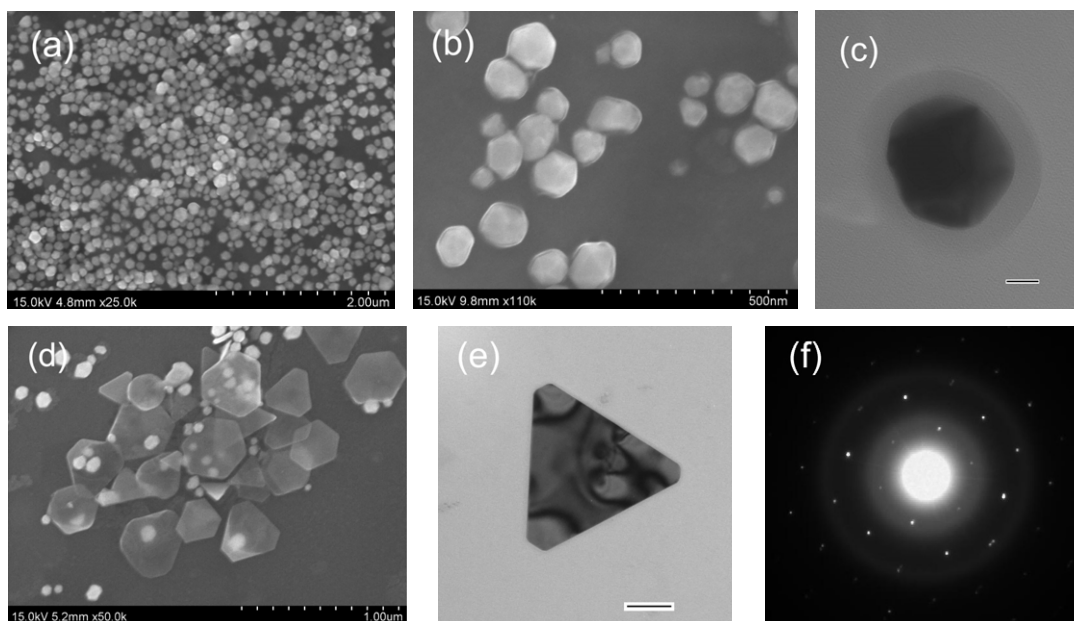


Figure 5. ((a), (b)) SEM images and (c) a TEM images (scale bar: 20 nm) of gold nanoparticles prepared from an aqueous solution of $\text{HAuCl}_4 \cdot 3\text{H}_2\text{O}$ and **Den 40** with concentrations of 40×10^{-5} and $4.20 \times 10^{-5} \text{ mol l}^{-1}$, respectively. (d) An SEM image for the large single crystals prepared from an aqueous solution of $\text{HAuCl}_4 \cdot 3\text{H}_2\text{O}$ and **Den 40** with concentrations of 32.50×10^{-5} and $4.20 \times 10^{-5} \text{ mol l}^{-1}$, respectively. (e) A TEM image (scale bar: 100 nm) of an individual large single crystal from (d), and (f) an ED pattern of (e). Note that all of the nanoparticles co-existed in the aqueous phase with the ribbon-like microfiber precipitates shown in figure 6.

ultrathin single crystals (figure 5), such as those produced by electrochemical syntheses of gold nanoparticles in the presence of poly(*N*-vinylpyrrolidone) (PVP) [41], were found to co-

exist with precipitated ribbon-like microfiber clusters (figure 6) in the aqueous solutions of **Den 40** and $\text{HAuCl}_4 \cdot 3\text{H}_2\text{O}$ at a relatively low ratio of **Den 40** to HAuCl_4 (<0.5). The

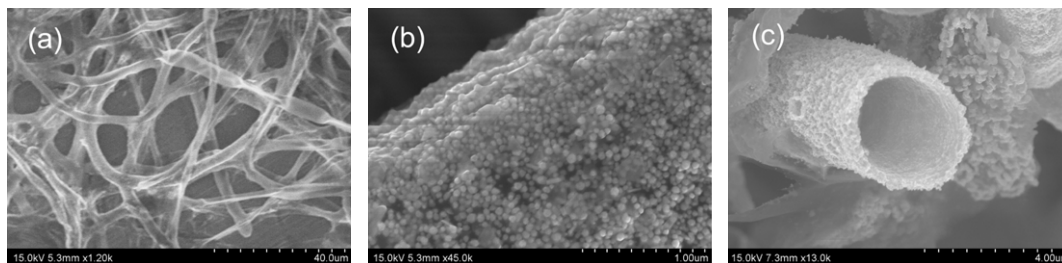


Figure 6. (a) A typical SEM image of the self-assembled microfiber, (b) as for (a) under a higher magnification, and (c) a cross-sectional view of an individual microfiber. The concentrations of $\text{HAuCl}_4 \cdot 3\text{H}_2\text{O}$ and **Den 40** are 24.40×10^{-5} and $4.20 \times 10^{-5} \text{ mol l}^{-1}$, respectively.

observed formation of large single crystals (figure 5), most likely results from the recrystallization and fusion of small particles into large ones because of an insufficient amount of the protecting/stabilizing agent (i.e. **Den 40** in this particular case). The TEM image of the gold nanoparticles given in figure 5(c) clearly shows the polyhedral geometry. Figure 5(c) further shows a thin surface layer, most probably arising from the residual dendrimers and/or photodegraded dendritic fragments coated on some of the sharp facets of the gold nanoparticle. An electron diffraction pattern for the large gold nanocrystal shown in figure 5(e) is given in figure 5(f), which shows a unique spot array, arising from the {111} orientation of the platelet lying flat on the substrate with the top facet perpendicular to the electron beam. Similar results were obtained for **Den 20** and **Den 30**, though the [Dendrimer]/[HAuCl_4] ratio for the transition from the stable to aggregated dispersion of gold nanoparticle increased slightly with decreasing their molecular weights from **Den 40** through **Den 30** to **Den 20**.

We have also found that the relatively large gold nanoparticles aggregated into interesting ribbon-like microfibers (about 1–4 μm in diameter, figure 6(a)) with a large number of gold nanoparticles (about 50 nm in diameter) aggregated on the fiber surface (figure 6(b)). Furthermore, the cross-sectional SEM image shows a hollow structure for the self-assembled fibers. In view of previous work on wire-/ribbon-like assemblies formed by certain nanoparticles and conjugated polymers [42], we envisaged that it is the selective adsorption of the conjugated dendritic moieties onto specific crystal faces of the gold nanoparticles (*supra infra*) that generates the dipolar moment required for self-assembling of the nanoparticles into the observed microfibers [43], though some further work is needed to understand the detailed mechanism governing the hollow microfiber formation. These newly formed gold nanoparticle self-assemblies stabilized with optoelectronic active dendritic segments with peculiar structures (e.g. hollow tubes) could spur unforeseen effort in the field.

4. Conclusions

In summary, we have demonstrated a new synthetic approach for the preparation of gold nanoparticles at ambient temperature by the photo-induced reduction of Au^{3+} ions in the presence of $\text{HAuCl}_4 \cdot 3\text{H}_2\text{O}$ and amphiphilic dendrimers with oligo(*p*-phenylenevinylene) core branches and oligo(ethylene oxide) terminal chains. Optical absorption and photoluminescent emission spectroscopic measurements,

together with SEM and TEM studies, revealed that the formation of Au nanoparticles in the present study resulted from the reduction of Au^{3+} ions by α -hydroxy methyl radicals photo-generated from the amphiphilic dendrimers. Both the concentration and molar ratio of the amphiphilic dendrimer to $\text{HAuCl}_4 \cdot 3\text{H}_2\text{O}$ played important roles in regulating the size/shape of the resultant nanoparticles and their subsequently self-assembled structures. In particular, it was shown that stable aqueous colloids of gold nanoparticles formed at high molar ratios of the amphiphilic dendrimer to HAuCl_4 (>0.5) whereas relatively large gold single-crystal films and self-assembled hollow fiber clusters were prepared at lower molar ratios of the amphiphilic dendrimer to HAuCl_4 . This newly developed simple, but versatile, approach could offer a wide range of potential possibilities for synthesizing various size/shaped controlled metal nanoparticles and their assemblies.

Acknowledgments

This work was supported by NSF (CMMI-0708055) under the Nanoscale Exploratory Research (NER) program, AFOSR (FA9550-06-1-0384), and WBI. The authors thank Dr Jianwei Liu and Ms Amanda Schrand for their help with TEM and ED measurements.

References

- [1] Lam D M K and Rossiter B W 1991 *Sci. Am.* **265** 80
Qu L and Dai L 2005 *J. Chem. Phys. B* **109** 13985
- [2] Goldstein A N (ed) 1997 *Handbook of Nanophase Materials* (New York: Dekker)
Dai L (ed) 2006 *Carbon Nanotechnology: Recent Developments in Chemistry, Physics, Materials Science and Device Applications* (Amsterdam: Elsevier)
Fendler J H (ed) 1998 *Nanoparticles and Nanostructured Films* (Weinheim: Wiley-VCH)
Feldheim D L and Colby A F (ed) 2002 *Metal Nanoparticles—Synthesis, Characterization and Applications* (New York: Dekker)
- [3] Faraday M 1857 *Phil. Trans.* **147** 145
Schmid G 1992 *Chem. Rev.* **92** 1709
Nakao Y and Kaeriyama K 1986 *J. Colloid Interface Sci.* **110** 82
Hirai H 1979 *J. Macromol. Sci. Chem.* **A13** 663
Qu L and Dai L 2005 *J. Am. Chem. Soc.* **127** 1080
- [4] Sun Y and Xia Y 2002 *Science* **298** 2176
Im S H, Lee Y T, Wiley B and Xia Y 2005 *Angew. Chem. Int. Edn* **44** 2154
Yu D and Yam V W 2004 *J. Am. Chem. Soc.* **126** 13200

- [5] Dumestre F, Chaudret B, Amiens G, Renaud P and Fejes P 2004 *Science* **303** 821
- [6] Wang W, Huang Y and Ren Z 2005 *Langmuir* **21** 751
- [7] Rao J, Zhang X, Qin B and Fung K 2003 *Phil. Mag. Lett.* **83** 395
- [8] Ren X, Chen D and Tang F 2005 *J. Phys. Chem. B* **109** 15803
- [9] Ahmadi T S, Wang Z L, Green T C, Henglein A and El-Sayed M A 1996 *Science* **272** 1924
- Ahmadi T S, Wang Z L, Green T C, Henglein A and El-Sayed M A 1996 *Chem. Mater.* **8** 1161
- [10] Song H, Kim F, Connor S, Somorjai G A and Yang P 2005 *J. Phys. Chem. B* **109** 188
- Kim F, Connor S, Song H, Kuykendall T and Yang P 2004 *Angew. Chem. Int. Edn* **43** 3673
- Xiong Y J, Chen J Y, Wiley B, Xia Y N, Yin Y D and Li Z Y 2005 *Nano Lett.* **5** 1237
- Qu L, Dai L and Osawa E 2006 *J. Am. Chem. Soc.* **128** 5523
- [11] Daniel M C and Astruc D 2004 *Chem. Rev.* **104** 293
- Roucoux A, Schulz J and Patin H 2002 *Chem. Rev.* **102** 3757
- Hayat M A 1989 *Colloidal Gold, Principles, Method, Applications* (New York: Academic)
- [12] Mandal M, Ghis S K, Kundu S, Esumi K and Pal T 2002 *Langmuir* **18** 7792
- Esumi K, Suzuki A, Aihara N, Usui K and Torigoe K 1998 *Langmuir* **14** 3157
- Gao J, Bender C M and Murphy C J 2003 *Langmuir* **19** 9065
- Sau T K and Murphy C J 2004 *J. Am. Chem. Soc.* **126** 8648
- Kuo C H and Huang M H 2005 *Langmuir* **21** 2012
- [13] Brust M, Walker M, Bethell D, Schiffrin D J and Whyman R J 1994 *Chem. Commun.* 801
- Frens G 1973 *Nature (Phys. Sci.)* **241** 20
- [14] Rotello V A (ed) 2004 *Nanoparticles: Building Blocks for Nanotechnology* (New York: Kulwer Academic/Platinum Publisher)
- Schimid G (ed) 1994 *Clusters and Colloid* (Weinheim: Wiley-VCH)
- [15] Hostetler M J, Green S J, Stokes J J and Murray R W 1996 *J. Am. Chem. Soc.* **118** 4212
- Chen S and Murray R W 1999 *Langmuir* **15** 682
- [16] Kuo C H, Chiang T F, Chen L J and Huang M H 2004 *Langmuir* **20** 7820
- Jana N R, Gearheart L and Murphy C J 2001 *Chem. Mater.* **13** 2313
- Deng J P, Wu C, Yang G H and Mou C Y 2005 *Langmuir* **21** 8947
- [17] Walker C H, John J V and Neilson P W 2001 *J. Am. Chem. Soc.* **123** 3846
- Filali M, Meier M A R, Schubert U S and Gohy J F 2005 *Langmuir* **21** 7995
- [18] Esumi K, Hosoya T, Suzuki A and Torigoe K 2000 *Langmuir* **16** 2978
- Zhao M, Sun L and Crooks R M 1998 *J. Am. Chem. Soc.* **120** 4877
- Crooks R M, Zhao M, Sun L, Chechik V and Yeung L K 2001 *Acc. Chem. Res.* **34** 181
- Wilson O M, Scott R W J, Garcia-Martinez J C and Crooks R M 2005 *J. Am. Chem. Soc.* **127** 1015
- [19] Sun X, Jiang X, Dong S and Wang E 2003 *Macromol. Rapid Commun.* **24** 1024
- [20] Zhou Y, Itoh H, Uemura T, Naka K and Chujo Y 2001 *Chem. Commun.* 61
- [21] Longenberger L and Mills G 1995 *J. Phys. Chem.* **99** 47
- [22] Sakai T and Alexandridis P 2004 *Langmuir* **20** 8426
- Sakai T and Alexandridis P 2005 *Langmuir* **21** 8019
- Sakai T and Alexandridis P 2005 *J. Phys. Chem. B* **109** 7766
- [23] Tano T, Esumi K and Meguro K 1989 *J. Colloid Interface Sci.* **133** 530
- Esumi K, Sadakane O, Torigoe K and Meguro K 1992 *Colloids Surf.* **62** 255
- [24] Mayer A B R and Mark J E 1998 *Eur. Polym. J.* **34** 103
- Zhou Y, Yang C Y, Zhu Y R and Chen Z Y 1999 *Chem. Mater.* **11** 2310
- Esumi K and Torigoe K 1992 *Langmuir* **8** 59
- Zhang L, Jimmy C Y, Yip H Y, Li Q, Kwong K Y, Xu A W and Wong P K 2003 *Langmuir* **19** 10372
- Kim F, Song H and Yang P 2002 *J. Am. Chem. Soc.* **124** 14316
- Mallick M, Witcomb M J and Scurrall M S 2005 *Appl. Phys. A* **80** 395
- [25] Suslick K S, Choe S B, Cichowlas A A and Grinstaff M W 1991 *Nature* **353** 414
- Fujimoto T, Terauchi S, Umehara H, Kojima I and Henderson W 2001 *Chem. Mater.* **13** 1057
- Okitsu K, Bandow H, Maeda Y and Nagata Y 1996 *Chem. Mater.* **8** 315
- [26] Reetz M T and Helbig W 1994 *J. Am. Chem. Soc.* **116** 7401
- Reetz M T and Quaiser S A 1995 *Angew. Chem. Int. Edn* **34** 2240
- [27] Burroughes J H, Bradley D D C, Brown A R, Marks R N, Mackay K, Friend R H, Burns P L and Holmes A B 1990 *Nature* **347** 539
- [28] Dai L and Mau A W H 2001 *Adv. Mater.* **13** 899
- Winkler B, Dai L and Mau A W H 1999 *Chem. Mater.* **11** 704
- [29] Ding L, Chang D W, Dai L, Ji T, Li S, Lu L, Yao Y, Delozier D and Connel J 2005 *Macromolecules* **38** 9389
- Ji T, Li S, Chang D W and Dai L 2006 *Synth. Met.* **156** 392
- [30] Dai L 2004 *Intelligent Macromolecules for Smart Devices: From Materials Synthesis to Device Applications* (Berlin: Springer)
- Harrison N T, Hayes G R, Philips R T and Friend R H 1996 *Phys. Rev. Lett.* **77** 1881
- Lin K K, Chua S J and Wang W 2002 *Thin Solid Films* **417** 36
- [31] Cumpston B H and Jensen K F 1995 *Chem. Commun.* **73** 195
- Dam N, Scurlock R D, Wang B, Ma L, Sundahl M and Ogilby P R 1999 *Chem. Mater.* **11** 1302
- Ma L *et al* 2002 *Chem. Phys.* **285** 85
- [32] Korchev A S, Bozack M J, Slanten B L and Mills G 2004 *J. Am. Chem. Soc.* **126** 10
- Korchev A S, Konovalova T, Cammarata V, Kispert L, Slaten L and Mills G 2006 *Langmuir* **22** 375
- Korchev A S, Shulyak T S, Slanten B L, Gale W E and Mills G 2005 *J. Phys. Chem. B* **109** 7733
- [33] Chang D W and Dai L 2007 *J. Mater. Chem.* **17** 364
- [34] Plater M J and Jackson T 2003 *Tetrahedron* **59** 4673
- Meier H and Lehman M 1998 *Angew. Chem. Int. Edn* **110** 643
- [35] Gerald J, Holzenkamp U and Meier H 2001 *Eur. J. Org. Chem.* **14** 2757
- [36] Mie G 1908 *Ann. Phys.* **25** 377
- [37] Link S and El-Sayed M A 1999 *J. Phys. Chem. B* **103** 8410
- [38] Goldstein A N (ed) 1997 *Handbook of Nanophase Materials* (New York: Dekker)
- [39] Thomas K G and Kamat P V 2003 *Acc. Chem. Res.* **36** 888
- [40] Herrikhuizen J, Janssen R A J, Meijer E W, Meskers S C J and Schenning A P H J 2006 *J. Am. Chem. Soc.* **128** 686
- [41] Huang S, Ma H, Zhang X, Yong F, Feng X, Pan W, Wang W, Wang Y and Chen S 2005 *J. Phys. Chem. B* **109** 19823
- [42] Zhang X, Zhang J, Song W and Liu Z 2006 *J. Phys. Chem. B* **110** 1158
- [43] Tang Z, Kotov N A and Giersig M 2002 *Science* **297** 237